In silico, in vitro, and in vivo models reveal EPHA2 as a target for decreasing inflammation and pathological endochondral ossification in osteoarthritis.

Mauricio N. Ferrao Blanco [1], Raphaelle Lesage [2,3], Nicole Kops [1], Niamh Fahy [1, 4, *], Fjodor T. Bekedam [1], Athina Chavli [1], Yvonne M. Bastiaansen-Jenniskens [1], Liesbet Geris [2,3,5], Mark G. Chambers [6], Andrew A. Pitsillides [7], Roberto Narcisi [1], Gerjo J.V.M. van Osch [1,8,9]

[1] Department of Orthopaedics and Sports Medicine, Erasmus MC, University Medical Center Rotterdam, Rotterdam, The Netherlands.

[2] Prometheus, Division of Skeletal Tissue Engineering, KU Leuven, Belgium.

[3] Biomechanics Section, KU Leuven, Belgium.

[4]Department of Oral and Maxillofacial Surgery, Erasmus MC, University Medical Center Rotterdam, Rotterdam, The Netherlands.

[*] Current affiliation. Department of Applied Science, Technological University of the Shannon: Midlands Midwest, Limerick, Ireland.

[5] GIGA In silico medicine, University of Liège, Belgium.

[6] Lilly Research Laboratories, Eli Lilly Pharmaceuticals, Indianapolis, USA.

[7] Comparative Biomedical Sciences, Royal Veterinary College, London, United Kingdom.

[8] Department of Otorhinolaryngology, Erasmus MC, University Medical Center Rotterdam, Rotterdam, The Netherlands.

[9] Department of Biomechanical Engineering, University of Technology Delft, Delft, The Netherlands.

Corresponding author: Gerjo J.V.M. van Osch, Erasmus MC, University Medical Center Rotterdam, Dr. Molewaterplein 40, Room Ee 16.55, 3015 GD Rotterdam, The Netherlands. Tel: +31-107043661.

Abstract

Low-grade inflammation and pathological endochondral ossification are processes underlying the progression of osteoarthritis, the most prevalent joint disease worldwide. In this study, data mining on publicly available transcriptomic datasets revealed EPHA2, a receptor tyrosine kinase associated with cancer, to be associated with both inflammation and endochondral ossification in osteoarthritis. A computational model of cellular signaling networks in chondrocytes predicted that in silico activation of EPHA2 in healthy chondrocytes increases inflammatory mediators and triggers hypertrophic differentiation, the phenotypic switch characteristic of endochondral ossification. We then evaluated the effect of inhibition of EPHA2 in cultured human chondrocytes isolated from individuals with osteoarthritis and demonstrated that inhibition of EPHA2 indeed reduced inflammation and hypertrophy. Additionally, systemic subcutaneous administration of the EPHA2 inhibitor ALW-II-41-27 attenuated joint degeneration in a mouse osteoarthritic model, reducing local inflammation and pathological endochondral ossification. Collectively, we demonstrate that pharmacological inhibition of EPHA2 with ALW-II-41-27 is a promising disease-modifying treatment that paves the way for a novel drug discovery pipeline for osteoarthritis.

Keywords: Chondrocyte hypertrophy, inflammation, kinase inhibitor, virtual cell, drug target

Author e-mails

Mauricio Nicolás Ferrao Blanco mauriferrao@gmail.com, Raphaelle Lesage lesage.raphaelle3@gmail.com, Nicole Kops n.kops@erasmusmc.nl, Niamh Fahy niamh.fahy@tus.ie, Fjodor T. Bekedam f.t.bekedam@amsterdamumc.nl, Athina Chavli athina.chav@gmail.com, Yvonne M. Bastiaansen-Jenniskens yvonne.bastiaansen@live.nl, Liesbet Geris liesbet.geris@kuleuven.be, Mark G. Chambers markchambers@lilly.com, Andrew A. Pitsillides apitsillides@rvc.ac.uk, Roberto Narcisi r.narcisi@erasmusmc.nl, Gerjo J.V.M. van Osch g.vanosch@erasmusmc.nl

Introduction

Osteoarthritis (OA) stands as the most widespread and debilitating musculoskeletal condition worldwide, characterized by progressive joint alterations leading to pain and functional limitations [1, 2]. In OA, joint inflammation ensues, resulting in the loss of cartilage lining the joint surface and the formation of bony outgrowths known as osteophytes at the joint edges. Current pharmacological treatments mainly focus on symptom management, primarily using pain relievers that do not impede disease advancement. Therefore, there is an imperative need to discover drugs capable of modifying OA progression.

Chondrocyte hypertrophy, a phenotype preceding cartilage calcification and eventual replacement by bone, plays a crucial role in OA pathogenesis. Under normal circumstances, articular chondrocytes resist hypertrophic changes. However, in OA, the onset of hypertrophic differentiation accelerates cartilage breakdown [3]. Similarly, joint margins are established through the growth of an initial cartilage template that undergoes endochondral ossification and is replaced by bone [4]. The inflammatory environment in OA, characterized by synovitis, involves heightened macrophage activation and the release of inflammatory cytokines like tumor necrosis factor-alpha (TNF-α) [5, 6]. Activation of inflammatory signaling pathways not only leads to cartilage matrix degradation but also triggers chondrocyte hypertrophy [7, 8].

Hence, we propose that targeting a key regulator governing both chondrocyte hypertrophy and inflammation could serve as an effective therapeutic approach for OA.

Methods

In silico simulations

A computational model of the intracellular signaling pathways regulating articular chondrocyte phenotypes was leveraged and completed with information about EPHA2 [9, 10]. In silico experiments involved setting targeted variables to specific values (0 for inhibition, 1 for activation) for 1,000 computing steps, followed by allowing variables to evolve freely until a new stable state was reached, simulating a bolus treatment effect. This process was repeated 100 times, and outcomes were averaged to compute final profiles and standard deviations. Four perturbations were applied: (1) EPHA2 activation, (2) pro-inflammatory cytokine activation, (3) combined activation of EPHA2 and pro-inflammatory cytokines, and (4) EPHA2 blockade with pro-inflammatory cytokine activation. The model and associated code are available via the following GitHub repository: https://github.com/Rapha-L/Virtual_Chondrocyte_for_EPHA2_study

Evaluation of ALW-II-41-27 in OA chondrocytes

In vitro validation was conducted using chondrocytes isolated from human articular cartilage obtained from OA donors (2 females, 1 male, aged 61, 64, and

115 69 years). Cartilage was obtained with implicit consent as waste material from
116 patients undergoing total knee replacement surgery, approved by the medical
117 ethical committee of the Erasmus MC, University Medical Center, Rotterdam
118 (protocol number MEC-2004-322). Cartilage chips were subjected to protease
119 and collagenase B digestion to isolate chondrocytes, which were then expanded
120 in monolayer culture. For redifferentiation, chondrocytes were cultured in a 3D
121 alginate bead model [11, 12]. After two weeks, cells were treated with 10 μM of
122 ALW-II-41-27, vehicle (DMSO), and/or TNF-α for 24 hours. Medium and
123 alginate beads were harvested for further analyses.
124

125 **Animal model**

126 All animal experimentation procedures were conducted in compliance with the
127 Animal Ethical Committee of Erasmus University Medical Center (License
128 number AVD101002015114, protocol number 16-691-06). Twelve-week-old
129 male C57BL/6 mice (C57BL/6J0laHsd, 27.01 g ± 2.05 g; Envigo,
130 Cambridgeshire, UK) were group-housed in individually ventilated cages and
131 maintained on a 12-hour light/dark cycle with unrestricted access to standard diet
132 and water at the Experimental Animal Facility of the Erasmus MC. Mice were
133 randomly assigned to two experimental groups (N=8 per group): Control and
134 ALW-II-41-27-treated mice.
135 For all procedures, mice were anesthetized using 3% isoflurane/0.8 L O2/min
136 (Pharmachemie BV, Haarlem, the Netherlands). Osteoarthritis (OA) was induced

137 unilaterally by intra-articular injections of 60 µg Monoiodoacetate (MIA)
138 (Sigma-Aldrich, St. Louis, USA) in 6 µl of saline (0.9% NaCl; Sigma-Aldrich)
139 on day 0. Injections were administered following a 3-4 mm dermal incision made
140 to the right knee at the height of the patellar tendon, using a 50 µl syringe
141 (Hamilton, Bonaduz, Switzerland) and 30G needle (BD Medical, New Jersey,
142 USA).
143 ALW-II-41-27 was administered via Alzet micro-osmotic pumps (Durect
144 Corporation, CA, USA) model 1004, with delivery rates of 0.11 µl/hour,
145 implanted subcutaneously on the back of the mice, slightly posterior to the
146 scapulae, immediately after the intra-articular injections. Osmotic pumps were
147 filled with dimethyl sulfoxide: polyethylene glycol alone (55:45 ratio, vehicle-
148 treated group, N=8 mice) or containing 6 mg of ALW-II-41-27 dissolved in
149 vehicle (treated group, N=8 mice), resulting in a dose of 6.6 µg/hour. A third
150 group of N=8 mice received osmotic pumps delivering a dose of 1.7 µg/hour of
151 ALW-II-41-27. A third group of N=8 mice received the implantation of osmotic
152 pumps delivering a dose of 1.7 µg/ hour of ALW-II-41-27. In the figures 5 and 6
153 we report the 6.6 µg/ hour dose of ALW-II-41-27. Synovial thickness, Krenn
154 score, and osteophyte size for all groups can be found in supplementary figure 6.
155 Mice were euthanized in accordance with Directive 2010/63/EU by cervical
156 dislocation under isoflurane anesthesia 14 days following MIA injection. Knee
157 specimens were fixed in 4% formalin (v/v) for 1 week, decalcified in 10% EDTA

158 for 2 weeks, and embedded in paraffin. Coronal sections of 6 μm were cut for
159 analysis.
160
161 **Data and statistical analyses**
162 Statistical analysis was conducted using GraphPad Prism 9.0 and IBM SPSS 24
163 (IBM). Each *in vitro* experiment comprised a minimum of 3 biological replicates
164 and was replicated using cells obtained from 3 donors. The *in vivo* study was
165 designed to ensure equal-sized groups, employing randomization and blinded
166 analyses. The stated group size represents the number of independent values used
167 for statistical analysis. Sample size for the *in vivo* study was determined based on
168 the distribution of weight over the hind limbs as read-out parameter. Based on
169 previous studies, we consider an increase of 13% (standard deviation of 10%) in
170 weight distribution on the affected limb in time in the therapy groups as relevant
171 in our study [13]. Sample size calculation was performed with a statistical power
172 of 80% and a significance level of 0.05, resulting in N=8.
173 For statistical analysis, a linear mixed model with Bonferroni's multiple
174 comparisons test was utilized.
175
176
177
178
179

180 **Results**

181 ***EPHA2* is as an inflammation-related gene upregulated in hypertrophic**
182 **chondrocytes and osteoarthritic cartilage**

183 To identify a new therapeutic target for OA linked with chondrocyte hypertrophy
184 and inflammation, we conducted data analysis on two publicly available murine
185 microarray datasets [14, 15]. Differentially expressed genes (DEGs) in the
186 articular cartilage of mice with OA induced by destabilization of the medial
187 meniscus (DMM) were compared to those from mice undergoing sham surgery,
188 identifying OA-related genes. By intersecting this set with DEGs in the
189 hypertrophic zone versus the proliferative zone of the mouse growth plate, we
190 identified 172 genes differentially expressed in OA associated with chondrocyte
191 hypertrophy. Among these, nine genes were associated with the gene ontology
192 inflammatory response [16] (Figure 1 A & B). Subsequently, we examined the
193 expression of these nine genes in a human microarray dataset obtained from OA
194 and healthy articular cartilage [17], finding that three genes were also upregulated
195 in human OA cartilage (Figure 1 C). While *GJA1* and *PTGS2* have been
196 previously studied in the context of OA [18], *EPHA2*, a tyrosine kinase receptor,
197 has an undisclosed role in OA. *Epha2* was 30-fold upregulated in OA versus sham
198 mouse articular cartilage (adjusted p-value= 2E-02) [15], and 3-fold upregulated
199 in human OA versus healthy cartilage (adjusted p-value= 1E-08) [17].
200 Additionally, *Epha2* was 19-fold higher in the hypertrophic compared to the
201 proliferative zone of the murine growth plate (adjusted p-value= 1E-07) [14].

202

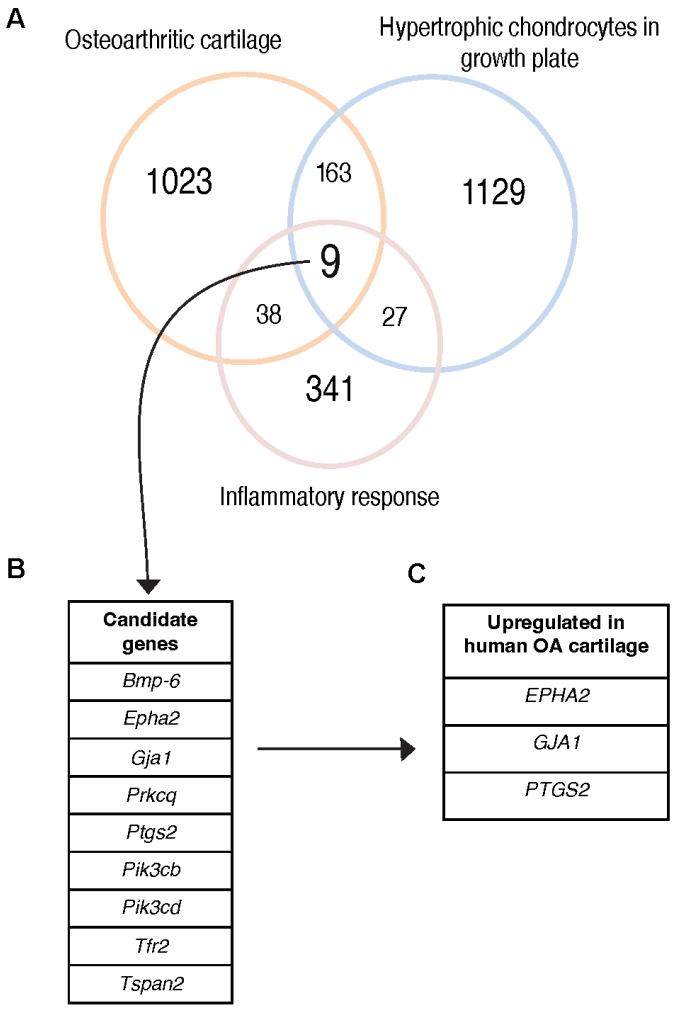
A
Osteoarthritic cartilage
Hypertrophic chondrocytes in growth plate
1023
163
1129
9
38
27
341
Inflammatory response
B
Candidate genes
Bmp-6
Epha2
Gja1
Prkcq
Ptgs2
Pik3cb
Pik3cd
Tfr2
Tspan2
C
Upregulated in human OA cartilage
EPHA2
GJA1
PTGS2

203

204

205 **Figure 1. Identification of EPHA2 as a novel target for OA associated with**
206 **inflammation and chondrocyte hypertrophy**. (A) The Venn diagram illustrates the
207 genes related to the inflammatory response, genes that were differentially regulated
208 in murine osteoarthritic cartilage (DMM vs sham) and genes differentially expressed
209 in the murine growth plate (proliferative vs hypertrophic zone). The number of genes
210 in each dataset is represented, together with those that overlapped. (B) List of 9
211 targets that overlapped in the three databases. (C) Target genes upregulated in
212 human OA compared with healthy articular cartilage. DEGs with a fold change greater
213 than 3, and an adjusted p value lower than of 0.05, were considered for the analysis.
214

215 **EPHA2 triggers inflammatory signaling activation and hypertrophy in a**
216 **virtual chondrocyte**

217 To assess the role of EPHA2 on chondrocyte phenotype we utilized a
218 computational model representing two cellular states: healthy and hypertrophic
219 chondrocytes (Figure 2 A) [9, 19]. EPHA2 exhibited activity in the hypertrophic
220 state but remained inactive in the healthy state (supplementary figure 1).
221 Activation of EPHA2 led to a more pronounced transition of healthy
222 chondrocytes towards the inflammatory hypertrophic state compared to
223 activation of inflammatory cytokines (9% and 5% for 'EPHA2+' and
224 'Inflammation+', respectively; Figure 2 B & C). Consequently, both conditions
225 prompted a decline in anabolic markers (collagen type II, Aggrecan: blue vs
226 orange and yellow bars; Figure 2 D) and an increase in hypertrophic and
227 inflammatory markers (Figure 2D & E). Full activation of both EPHA2 and

228 inflammatory cytokines synergistically induced a complete transition of healthy
229 chondrocytes towards the inflammatory hypertrophic state ('Inflammation+
230 EPHA2+'; Figure 2 C). Intriguingly, inhibiting EPHA2 (Inflammation+ EPHA2-
231) abolished this cellular state switching, accompanied by a significant reduction
232 in the activity of hypertrophic and inflammatory entities (green vs violet and
233 yellow bars; Figure 2 D & E). These computational findings substantiate the
234 hypertrophic and inflammatory role of EPHA2 in chondrocytes.
235

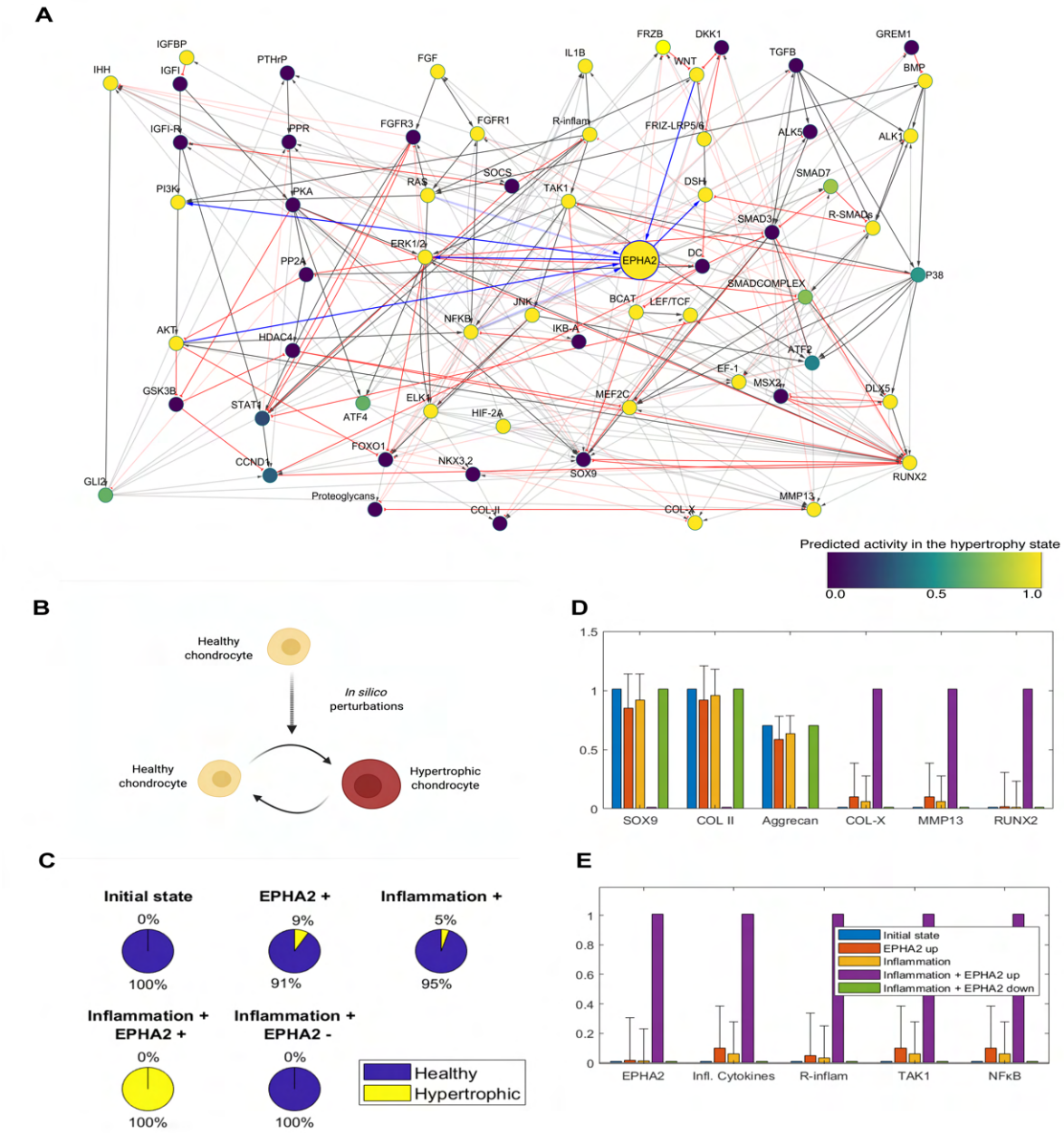

Figure 2. EPHA2 activation induces chondrocyte hypertrophy and inflammation in silico (A) Integration of EPHA2 in the regulatory network of articular chondrocytes. Solid lines denote protein interaction while modulation at the gene level is in dotted lines. Activating interactions are in grey with delta arrows and inhibitory interactions are in red with a half circle. Connections with EPHA2 are

243 denoted in blue. All components of the model are represented with a variable that
244 is named with capital letters. The variable represents neither the protein activation
245 level nor the gene expression but a product of both (global activity). The color of
246 the nodes in the network denotes the global activity of the variables in the
247 hypertrophic state, with dark blue being 0 and yellow being 1. (B) Effect of
248 gradually increasing the value of the EPHA2 input (from 0 to 1) in the scenario
249 with EPHA2 activation and Inflammation, on the chondrocyte state transition.
250 The initial state being the healthy (SOX9 +). (C) Activation of EPHA2 in the
251 healthy state promotes the transition to a hypertrophic phenotype. Forced
252 activation (+) or inhibition (-) of the entities from the initial healthy state is
253 shown. Inflammation represents the activation of the variables related to
254 inflammatory cytokines and their receptors, as input in the model. Pie charts
255 represent the predicted percentage of perturbations leading to a transition to the
256 hypertrophic phenotype or remaining in the healthy phenotype. (D) Average
257 activity of the chondrogenic markers, being type II collagen, Aggrecan and SRY-
258 box transcription factor (SOX9), and of hypertrophic markers, being Runt-related
259 transcription factor 2 (RUNX2), Matrix Metallopeptidase (MMP13) and type 10
260 Collagen. (E) Average activity of EPHA2 and variables associated with
261 inflammation. The bars represent the mean of the results of a hundred in silico
262 experiments (+ standard deviations, +SD). There is no SD for the initial state
263 (blue condition) as it denotes the starting point before the in silico perturbation is
264 applied. Figure created with Cytoscape, MATLAB and Biorender.com

265

266 **ALW-II-41-27 reduces human OA-derived chondrocyte inflammation**

267 To investigate the potential of pharmacologically inhibiting EPHA2 to alleviate
268 inflammation in OA, we utilized the tyrosine kinase inhibitor ALW-II-41-27, a
269 type II kinase inhibitor known for its high selectivity for EPHA2 [20, 21].
270 Initially, we validated the ability of ALW-II-41-27 to reduce TNF-α-induced
271 phosphorylation of EPHA2 in a dose-dependent manner (Figure 3 A). Notably,
272 the concentration of 10 micromolars exhibited the highest efficacy in decreasing
273 both EPHA2 phosphorylation and the expression of catabolic enzymes MMP1
274 and MMP13 in OA cartilage explants (supplementary figure 3). Subsequently,
275 we examined the effects of ALW-II-41-27 at a concentration of 10 micromolars
276 on TNF-α-treated human chondrocytes from OA donors (Figure 3 B). Treatment
277 with ALW-II-41-27 significantly inhibited TNF-α-induced inflammatory
278 responses, as evidenced by a reduction in the secretion of nitric oxide metabolites
279 (Figure 3 C). Furthermore, ALW-II-41-27 administration mitigated the TNF-α-
280 induced expression of the inflammatory cytokine interleukin (IL)-6, known to be
281 a downstream target of TNF-α (Figure 2 D & E) [22]. Moreover, ALW-II-41-27
282 treatment countered the TNF-α-induced upregulation of the cartilage matrix-
283 degrading enzymes MMP1 and MMP13 (Figure 3 F & G). These findings
284 demonstrate the anti-inflammatory potential of ALW-II-41-27 in TNF-α-
285 stimulated OA chondrocytes.

286

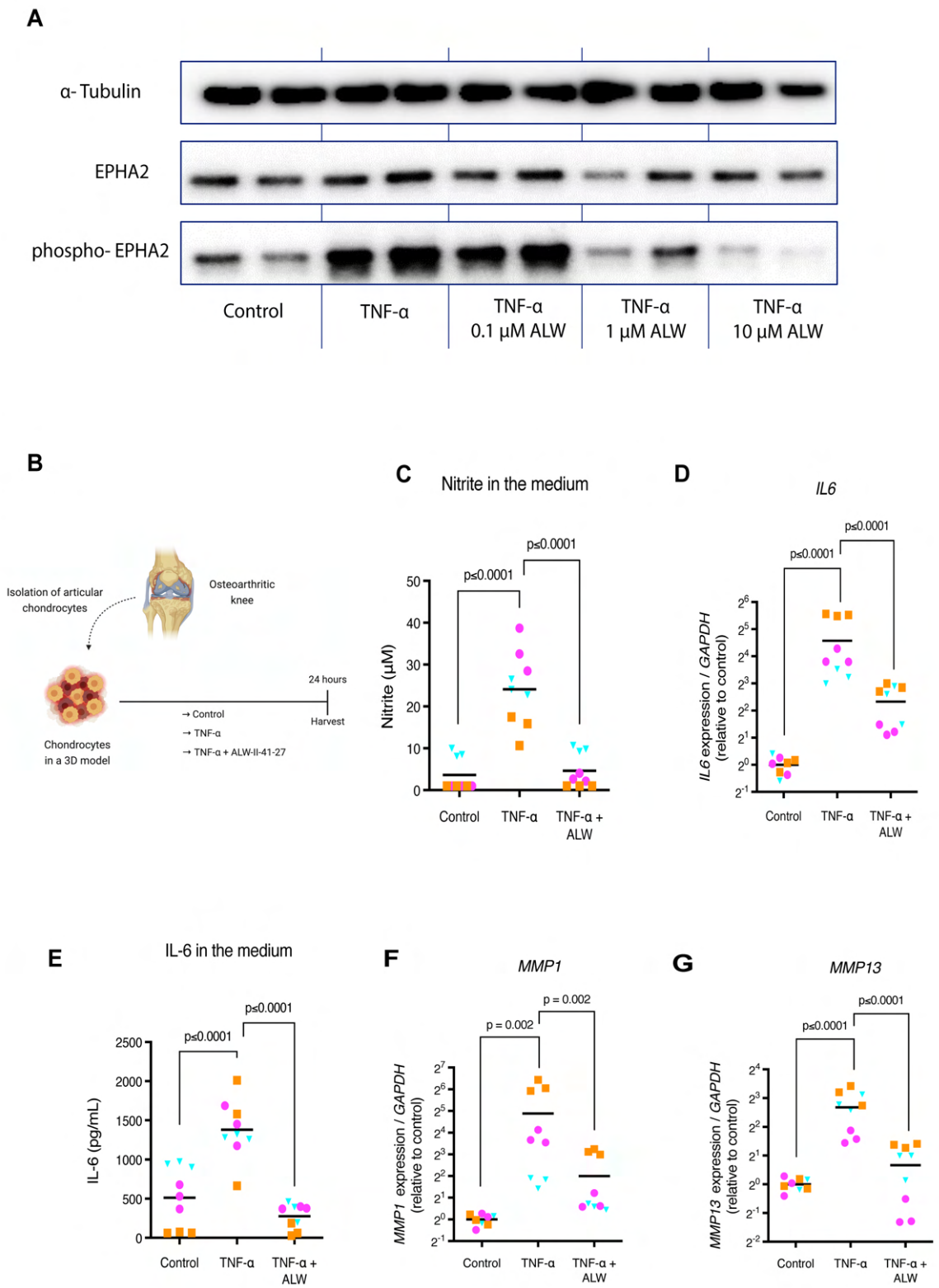
A
α- Tubulin
EPHA2
phospho- EPHA2
Control
TNF-α
TNF-α 0.1 µM ALW
TNF-α 1 µM ALW
TNF-α 10 µM ALW
B
Isolation of articular chondrocytes
Osteoarthritic knee
Chondrocytes in a 3D model
24 hours
Harvest
→ Control
→ TNF-α
→ TNF-α + ALW-II-41-27
C
Nitrite in the medium
Nitrite (µM)
p≤0.0001
p≤0.0001
Control
TNF-α
TNF-α + ALW
D
IL6
IL6 expression / GAPDH (relative to control)
p≤0.0001
p≤0.0001
Control
TNF-α
TNF-α + ALW
E
IL-6 in the medium
IL-6 (pg/mL)
p≤0.0001
p≤0.0001
Control
TNF-α
TNF-α + ALW
F
MMP1
MMP1 expression / GAPDH (relative to control)
p = 0.002
p = 0.002
Control
TNF-α
TNF-α + ALW
G
MMP13
MMP13 expression / GAPDH (relative to control)
p≤0.0001
p≤0.0001
Control
TNF-α
TNF-α + ALW

287

288

289 Figure 3. ALW-II-41-27 decreases TNF-α induced catabolism and inflammation
290 in human chondrocytes. (A) ALW-II-41-27 decreases TNFα-induced
291 phosphorylation of EPHA2 in a dose-dependent manner. (B) Experimental set-
292 up to evaluate the anti-inflammatory capacity of ALW-II-41-27 (10 μM) in
293 human OA chondrocytes cultured with 10 ng/mL TNF-α. (C) Evaluation of
294 nitrite in the medium as a marker for inflammatory activity as determined by
295 Griess reagent. (D, F-G) Gene expression of IL6, MMP1 and MMP13 determined
296 by qPCR. The average of control, per donor, is set to 1. (E) IL-6 in the medium
297 determined by ELISA. Experiments were performed in triplicate, with cells from
298 three donors. Donors are represented with different colors and symbols: violet
299 circles (donor 1), blue triangles (donor 2) and orange squares (donor 3). The
300 horizontal line in the graphs represents the mean. Data were analyzed with the
301 linear mixed model with Bonferroni's multiple comparisons test. Figure created
302 with Biorender.com
303

304 **ALW-II-41-27 decreases chondrocyte hypertrophy**

305 We then proceeded to evaluate whether pharmacological inhibition of EPHA2
306 with ALW-II-41-27 could impede hypertrophy in human OA-derived articular
307 chondrocytes (Fig. 4 A). ALW-II-41-27 decreased *COL10A1* expression (Figure
308 4 B), suggesting a reduction in hypertrophy. Given that chondrocyte hypertrophy
309 poses a significant obstacle to stable hyaline cartilage tissue engineering [23], we
310 further investigated the effect of ALW-II-41-27 on cartilage tissue engineered

311 constructs from mesenchymal stromal cells (MSCs), well-known to become
312 hypertrophic and prone to ossify when implanted *in vivo* [24-27] (Figure 4 C).
313 Gene expression analysis indicated that the addition of ALW-II-41-27 mitigated
314 the hypertrophic markers *COL10A1* and *ALPL* (Figure 4 D & E). Likewise, when
315 treated with ALW-II-41-27, the cells exhibited reduced deposition of type X
316 Collagen (Figure 4 F and supplementary figure 4). Intriguingly, neither
317 glycosaminoglycan nor type II Collagen deposition showed reduction, suggesting
318 that ALW-II-41-27 primarily targeted hypertrophy.
319

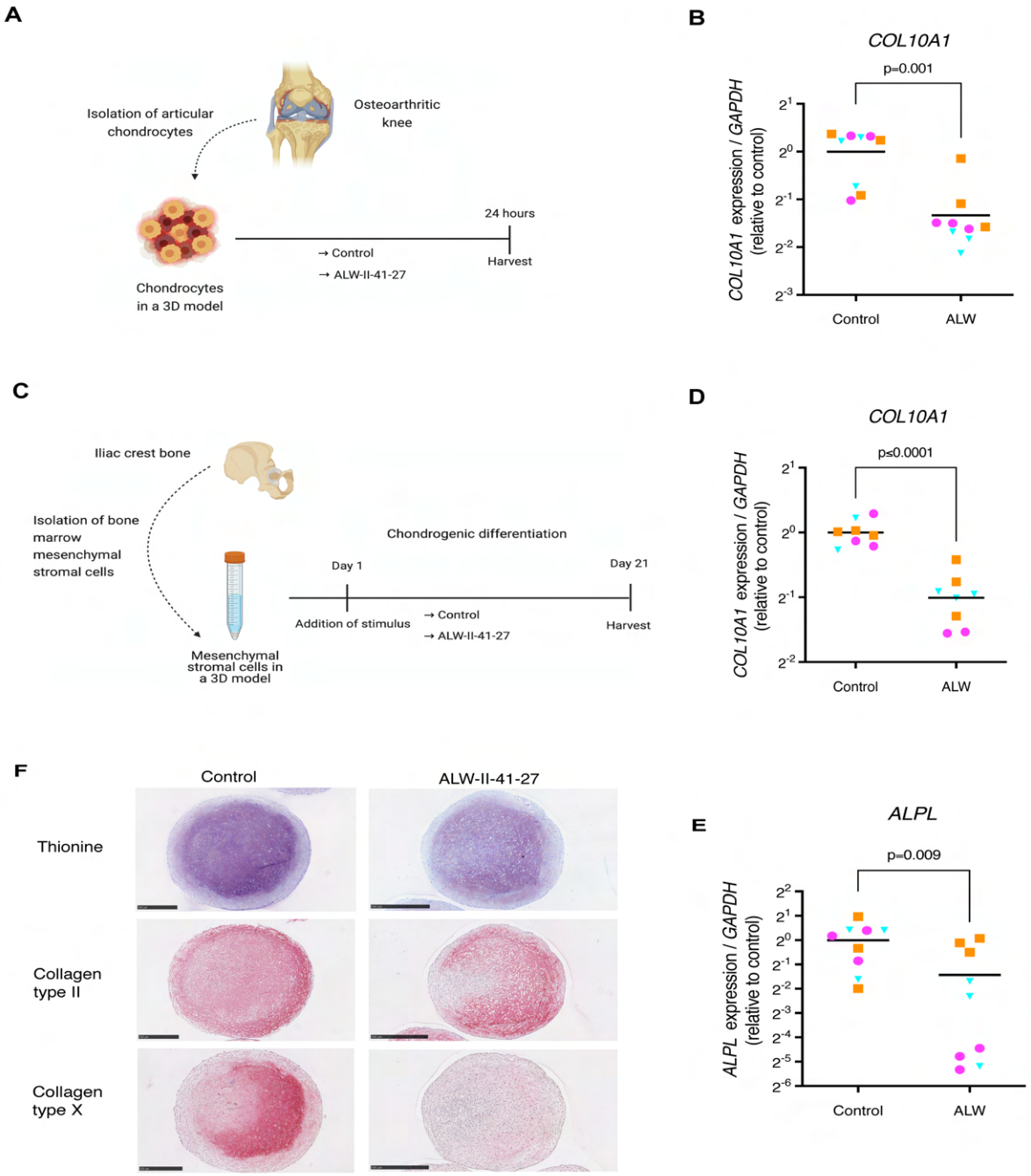

Figure 4. ALW-II-41-27 decreases chondrocyte hypertrophy. (A) Experimental set-up to evaluate the capacity of ALW-II-41-27 (10 µM) to modulate hypertrophy in human OA chondrocytes. (B) Gene expression of the hypertrophic marker COL10A1 in cultured OA chondrocytes determined by qPCR. (C)

326 Experimental set-up to evaluate how ALW-II-41-27 (100 nM) affects
327 hypertrophy in tissue engineered cartilage from MSCs. (D, E) Gene expression
328 of COL10A1 and ALPL in MSC-generated cartilage determined by qPCR. (F)
329 Histological analysis of tissue engineered cartilage derived from MSCs; Thionine
330 staining showing glycosaminoglycans (violet), and immunohistochemistry of
331 type II and type X collagen (red/pink). Experiments were performed with 3
332 replicates, for each of the three donors. Donors are represented with different
333 colors and symbols: violet circles (donor 1), blue triangles (donor 2) and orange
334 squares (donor 3). For gene expression analysis, the average of control replicates
335 is set to 1 per donor. The horizontal line in the graphs represents the mean. For
336 statistical analysis, the linear mixed model with Bonferroni's multiple
337 comparisons test was performed. Figure created with Biorender.com
338

339 **ALW-II-41-27 treatment reduces joint inflammation and pathological**
340 **endochondral ossification *in vivo***

341 EPHA2 inhibition reduced hypertrophy and inflammation *in silico* and its
342 pharmacological inhibition with ALW-II-41-27 in cell culture *in vitro* confirmed
343 these results. Subsequently, we sought to assess the potential therapeutic efficacy
344 of ALW-II-41-27 in vivo using a mouse model of joint pain and degeneration
345 induced by intra-articular injection of monoiodoacetate (MIA) [28]. ALW-II-41-
346 27 was administered subcutaneously with a controlled delivery system (Figure 5
347 A). Notably, the total body weight remained unaffected by ALW-II-41-27

348 administration throughout the 14-day study period, indicating no significant
349 adverse effects on the general health of the animals (supplementary figure 5).
350 Treatment with ALW-II-41-27 led to a reduction in synovial membrane thickness
351 and synovitis compared to vehicle-treated mice (Figure 5 B, C, D & E). Synovitis
352 is governed by macrophages, the crucial regulators of OA progression and
353 primary mediators of the inflammatory response [29, 30]. Macrophages were
354 solely observed in the synovial lining of vehicle-treated mice, suggesting
355 effective attenuation of joint inflammation (Figure 5 F). Moreover, there were no
356 discernible alterations in peripheral blood monocyte levels at day 2 and 12
357 (Figure 5 G), indicating selective reduction of local joint inflammation without
358 affecting systemic immune cells.
359 Despite joint pain being a significant OA symptom often associated with
360 inflammation [31], no significant difference in weight distribution between limbs
361 was detected between ALW-II-41-27-treated and vehicle-treated mice,
362 suggesting no apparent effect on pain (supplementary Figure 6).
363

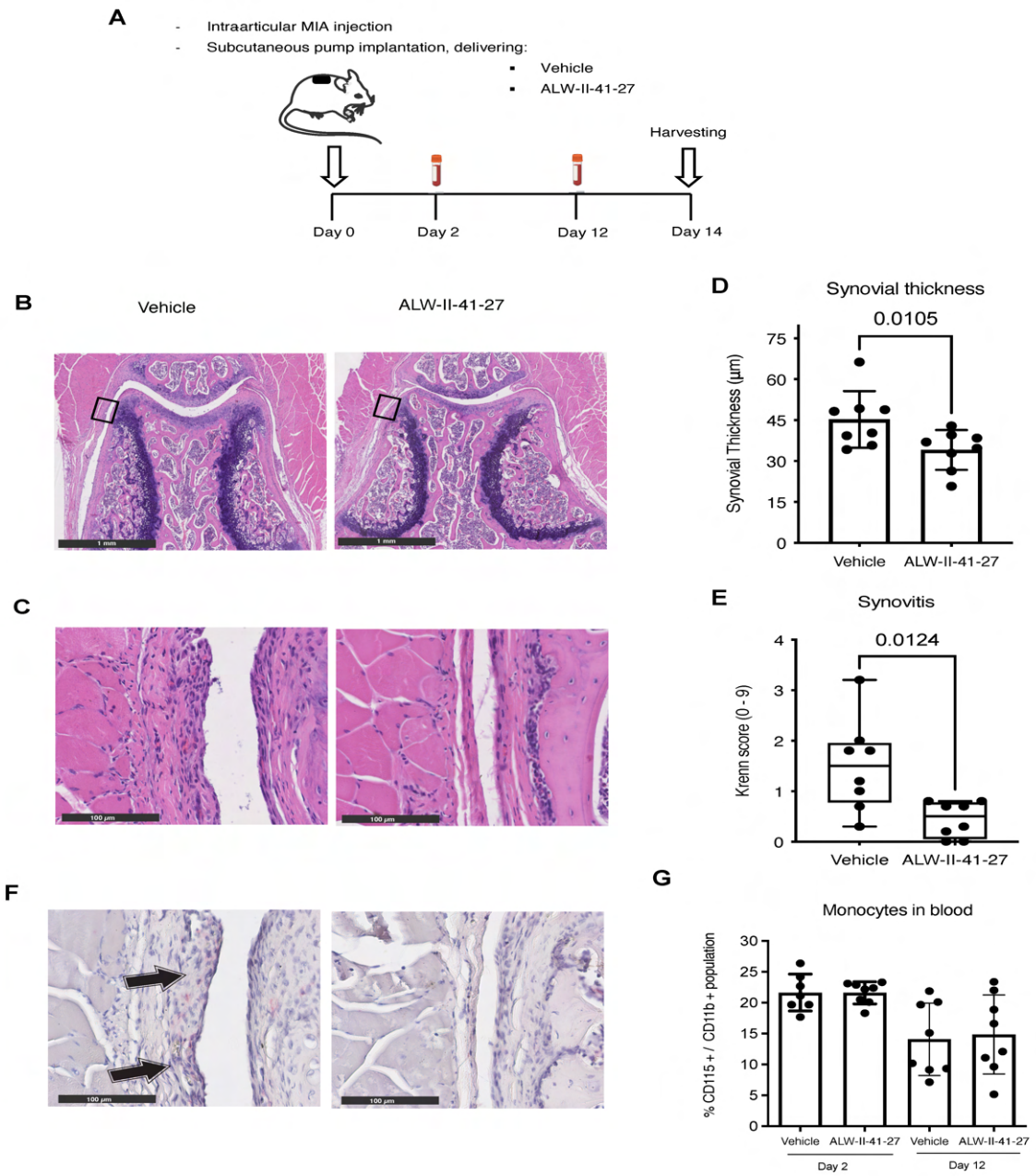

Figure 5. ALW-II-41-27 treatment attenuates joint inflammation. (A) Experimental set-up of the in vivo experiment. Intra-articular injection of monoiodoacetate (MIA, 60 µg in 6 µl of saline) was applied to the right knee of mice for each experimental group (N=8) to induce OA. An osmotic pump was implanted on the back of the mice, slightly posterior to the scapulae, which

371 continuously delivered vehicle or ALW-II-41-27 in a dose of 6.6 µg/ hour. At
372 day 2 and 12 peripheral blood was harvested. At day 14 mice were euthanized to
373 assess the effects of ALW-II-41-27 on the degenerated joint. (B) Hematoxylin
374 and Eosin staining of knees (patellofemoral region) from vehicle-treated and
375 ALW-II-41-27-treated mice. Black square indicates the region of magnification
376 for the image below (C) showing the synovial lining where synovial thickness
377 and Krenn score were determined. (D) Synovial thickness is represented by the
378 mean ± SD. (E) Krenn score illustrated with box-and-whiskers plots, with line
379 indicating the median and error bars spanning maximum to minimum values. (F)
380 Immunohistochemistry of F4/80 (pink) showing macrophages in the synovial
381 lining. Arrows indicate positive staining. (G) Percentage of monocytes present in
382 the peripheral blood of mice at day 2 and 12, respect to the myeloid cell
383 population. In all graphs, each dot represents data of an individual mouse (N=8).
384 For statistical analysis, the linear mixed model with Bonferroni's multiple
385 comparisons test was performed. Figure created with Biorender.com
386
387 Cartilage degeneration, evidenced by proteoglycan loss, was observed in all mice
388 irrespective of ALW-II-41-27 treatment (Figure 6 A & B), suggesting that ALW-
389 II-41-27 was not able to rescue matrix degeneration *in vivo*. However,
390 histological assessment revealed significantly smaller osteophytes, particularly at
391 the lateral side of the patella, in ALW-II-41-27-treated mice (Figure 6 C & D).
392 Additionally, type X collagen deposition was reduced in the knees of ALW-II-

393 41-27-treated mice (Figure 6 E), suggesting effective targeting of endochondral

394 ossification in the injured joint.

395

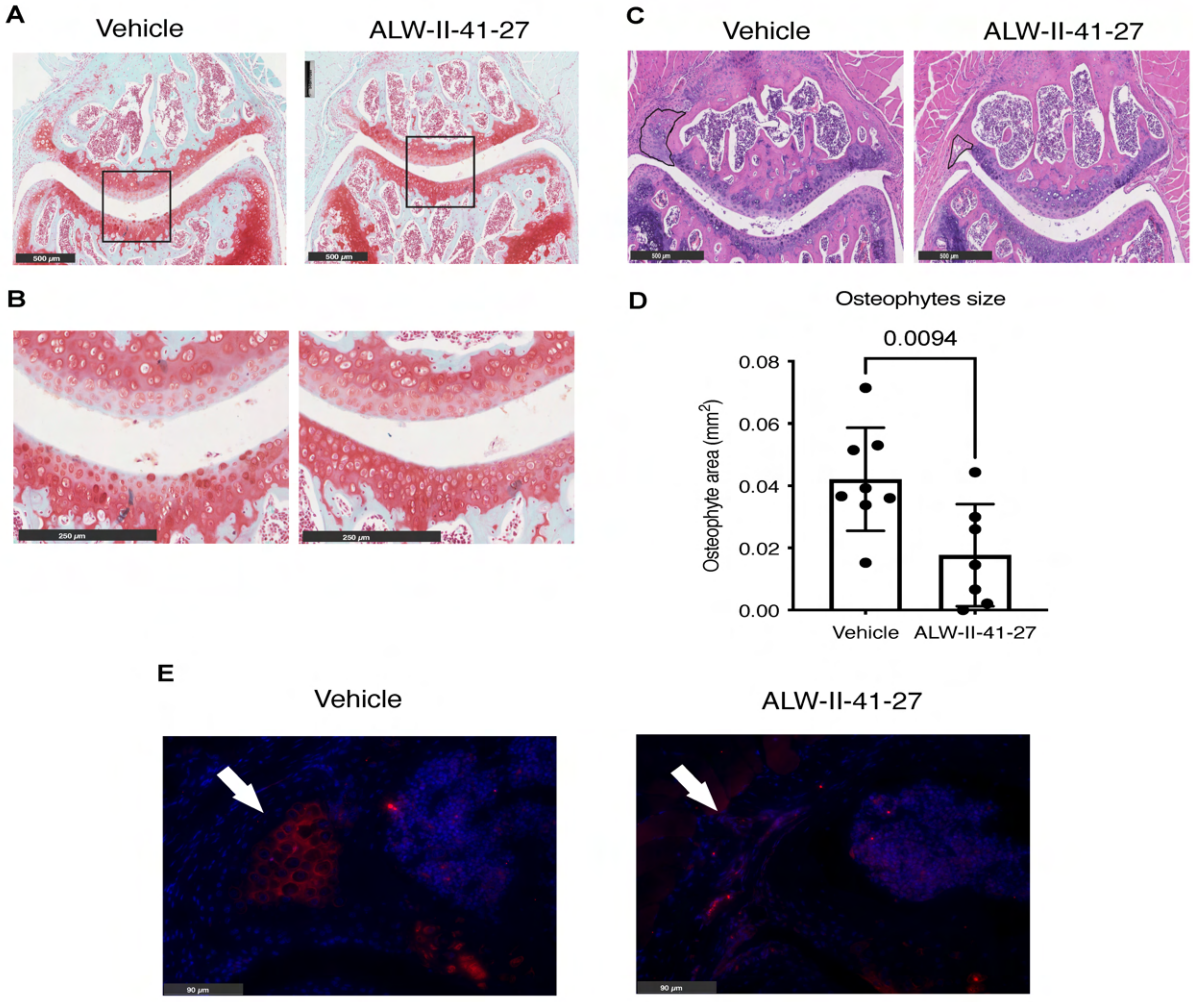

396

397

398 Figure 6. ALW-II-41-27 treatment attenuates pathological endochondral
399 ossification (A) Safranin-O / Fast Green staining of vehicle-treated and ALW-II-
400 41-27-treated mice knees with magnification of the patellofemoral region. Black
401 square indicates the region of magnification for the image below (B) showing the
402 central part of the patellofemoral articular cartilage. (C) Hematoxylin and Eosin
403 stain of vehicle-treated and ALW-II-41-27-treated mice knees with magnification
404 of the patellofemoral region. Osteophyte's diameter is indicated with a black line
405 in the lateral side of the patella. (D) Osteophyte area adjacent to the lateral side
406 of the patella is represented by the mean ± SD. Each dot represents data of an
407 individual mouse (n=8). For statistical analysis, the linear mixed model with
408 Bonferroni's multiple comparisons test was performed (E) Immunofluorescence
409 of type X collagen (red) and DAPI (blue) in the lateral side of the patellofemoral
410 region. Arrow indicates an osteophyte in the lateral side of the patella.
411
412
413
414
415
416
417
418
419

420 **Discussion**

421 There is an urgent unmet need for effective therapies for OA patients. Here, we
422 show that EPHA2 is a promising drug target for OA and we report the small
423 molecule ALW-II-41-27 as a disease-modifying OA drug (DMOAD),
424 specifically targeting inflammation and pathological endochondral ossification
425 (Fig. 7A). To find targets associated with inflammation and chondrocyte
426 hypertrophy we have used a particular sequence of studies that involved *in silico*,
427 *in vitro* and *in vivo* analyses (Figure 7 B). For the i*n silico* analyses we leveraged
428 previously published large gene expression dataset depositories and narrowed
429 them down to one target of interest. The role of the identified target on
430 inflammation and chondrocyte hypertrophy was further investigated through *in*
431 *silico* experiments using a computational model of cellular signaling networks
432 controlling chondrocyte phenotypes. These *in silico* studies served as the starting
433 point for a series of *in vitro* experiments using different cell models, which were
434 followed by an *in vivo* study. Our study illustrates the efficacy of this
435 experimental approach in uncovering a novel target for specific biological
436 processes in osteoarthritis

437 While previous research has implicated EPHA2 as a key player in diseases like
438 cancer [32-35] and irritable bowel disease [36], our study marks the first to
439 underscore its significance in OA. Other tyrosine kinases, including fibroblast
440 growth factor receptor (FGFR) 1, Fyn and vascular endothelial growth factor
441 receptor (VEGFR), have been implicated to promote chondrocyte hypertrophy

442 [37-40]. Our findings reveal that the tyrosine kinase EPHA2 not only contributes
443 to hypertrophy but also to inflammation, making it a compelling target for
444 mitigating pathological mechanisms in OA.
445 We have identified a promising compound, ALW-II-41-27, demonstrating
446 potential as a disease-modifying osteoarthritic drug (DMOAD). To date, a wide
447 variety of DMOADs targeting chondrocyte hypertrophy have been tested in
448 experimental pre-clinical studies [41-43]. It is unclear, however, whether those
449 agents have been subjected to further research. Regulatory agencies, such as the
450 Food and Drug Administration (FDA) or the European Medicines Agency
451 (EMA), have not yet approved any existing disease-modifying pharmacological
452 intervention for OA [44]. Considering the pre-clinical data of ALW-II-41-27 to
453 modulate OA pathogenesis and its extensive pharmacological analysis in other
454 conditions [32-36], it is expected that clinical trials involving this compound may
455 pose lower risks with a higher likelihood of success.
456 In addition to cartilage hypertrophy, inflammation of the synovium plays a crucial
457 role in OA pathology [45]. Our results indicate that ALW-II-41-27 exhibits anti-
458 inflammatory properties, aligning with its previously observed effects in a model
459 of irritable bowel syndrome [36]. EPHA2 is not limited to chondrocytes but is
460 also expressed in various other cell types found in the synovium, including
461 fibroblasts, monocytes, and macrophages [46, 47]. Thus, the observed anti-
462 inflammatory mechanism in our *in vivo* setting may also be linked to the action
463 of ALW-II-41-27 on these cell types.

464 Our study has certain limitations. Treatment initiation coincided with OA
465 induction in our research. This decision was influenced by the progressive nature
466 of the disease, posing a challenge for a DMOAD to reverse extensive joint
467 structural changes in end-stage OA. Hence, maximizing the pharmacological
468 benefits of ALW-II-41-27 to reduce inflammation and osteophytosis might be
469 more effective if administered during the earlier stages of the disease. Our study
470 did not demonstrate that *in vivo* administration of ALW-II-41-27 prevented
471 cartilage loss or pain in the MIA mouse model. Further investigation using
472 alternative experimental animal models is warranted to determine whether ALW-
473 II-41-27 specifically targets hypertrophy and inflammation, or if its effects extend
474 to preventing cartilage degeneration and alleviating pain. Additionally, exploring
475 the potential effects of ALW-II-41-27 on post-traumatic OA or other non-
476 chemically induced forms of OA is essential.
477 In conclusion, our findings suggest that EPHA2 contributes to the pathogenesis
478 of OA. The use of ALW-II-41-27 to inhibit EPHA2 showed promising results in
479 mitigating inflammation and pathological endochondral ossification across
480 various models, including *in silico* simulations, *in vitro* experiments with patient-
481 derived cells, and a mouse model. These results underscore the potential of ALW-
482 II-41-27 as a candidate drug for modifying the course of OA, warranting further
483 investigation.
484

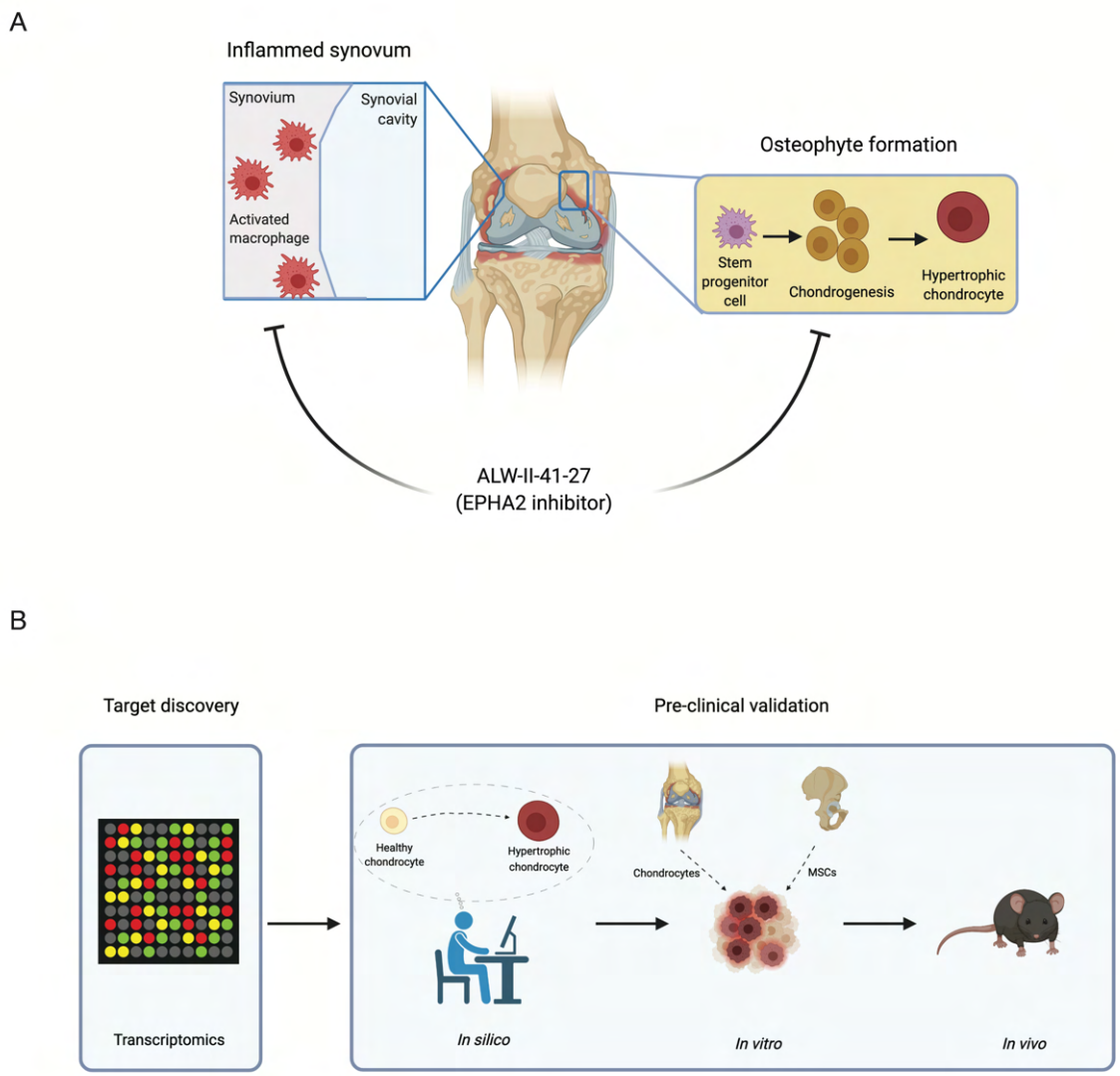

485

486

487 Figure 7. Graphical representation of main findings and experimental approach.

488 (A) ALW-II-41-27 attenuates synovitis and osteophyte formation. (B) Drug

489 discovery pipeline combining transcriptomic datasets, in silico, in vitro and in

490 vivo models. Figure created with Biorender.com

491

492 All authors approved the final version of the manuscript

Ethical statement

Animal experiments were approved by the medical ethical committee of the Erasmus MC, protocol EMC 16-691-06. Human articular cartilage was obtained with the approval of Erasmus MC, protocol MEC-2004-322 and mesenchymal stromal cells MEC-2014-16.

Funding

This study was financially supported by the European Union's Horizon 2020 research and innovation programme under the Marie Sklodowska-Curie grant agreement no. 721432 Carbon and the Reumafonds ReumaNederland grant number 18-1-202.

Supplementary methods

Description of further procedures can be found in supplementary methods.

Competing interest statement

The author(s) declared the following potential conflicts of interest with respect to the research, authorship, and/or publication of this article: M.G. Chambers is an employee of Eli Lilly but they did not fund this research.

References

1. Cross, M., et al., *The global burden of hip and knee osteoarthritis: estimates from the global burden of disease 2010 study.* Ann Rheum Dis, 2014. **73**(7): p. 1323-30.
2. Loeser, R.F., et al., *Osteoarthritis: a disease of the joint as an organ.* Arthritis Rheum, 2012. **64**(6): p. 1697-707.
3. van der Kraan, P.M. and W.B. van den Berg, *Chondrocyte hypertrophy and osteoarthritis: role in initiation and progression of cartilage degeneration?* Osteoarthritis Cartilage, 2012. **20**(3): p. 223-32.
4. Roelofs, A.J., et al., *Identification of the skeletal progenitor cells forming osteophytes in osteoarthritis.* Ann Rheum Dis, 2020. **79**(12): p. 1625-1634.
5. Smith, M.D., et al., *Synovial membrane inflammation and cytokine production in patients with early osteoarthritis.* J Rheumatol, 1997. **24**(2): p. 365-71.
6. Benito, M.J., et al., *Synovial tissue inflammation in early and late osteoarthritis.* Ann Rheum Dis, 2005. **64**(9): p. 1263-7.
7. Saito, T., et al., *Transcriptional regulation of endochondral ossification by HIF-2alpha during skeletal growth and osteoarthritis development.* Nat Med, 2010. **16**(6): p. 678-86.
8. Ferrao Blanco, M.N., et al., *Effect of Inflammatory Signaling on Human Articular Chondrocyte Hypertrophy: Potential Involvement of Tissue Repair Macrophages.* Cartilage, 2021. **13**(2_suppl): p. 168S-174S.
9. Lesage R, F.B.M., Narcisi R, Welting T, van Osch GJVM, Geris L., *An integrated in silico-in vitro approach for identifying therapeutic targets against osteoarthritis.* BMC Biology, 2022. **20**(1).
10. Kerkhofs, J., et al., *A Qualitative Model of the Differentiation Network in Chondrocyte Maturation: A Holistic View of Chondrocyte Hypertrophy.* PLoS One, 2016. **11**(8): p. e0162052.
11. Yaeger, P.C., et al., *Synergistic action of transforming growth factor-beta and insulin-like growth factor-I induces expression of type II collagen and aggrecan genes in adult human articular chondrocytes.* Exp Cell Res, 1997. **237**(2): p. 318-25.
12. Mandl, E.W., et al., *Multiplication of human chondrocytes with low seeding densities accelerates cell yield without losing redifferentiation capacity.* Tissue Eng, 2004. **10**(1-2): p. 109-18.
13. Yuan, X.C., et al., *Electroacupuncture potentiates peripheral CB2 receptor-inhibited chronic pain in a mouse model of knee osteoarthritis.* J Pain Res, 2018. **11**: p. 2797-2808.
14. Belluoccio, D., et al., *Sorting of growth plate chondrocytes allows the isolation and characterization of cells of a defined differentiation status.* J Bone Miner Res, 2010. **25**(6): p. 1267-81.
15. Bateman, J.F., et al., *Transcriptomics of wild-type mice and mice lacking ADAMTS-5 activity identifies genes involved in osteoarthritis initiation and cartilage destruction.* Arthritis Rheum, 2013. **65**(6): p. 1547-60.
16. Ashburner, M., et al., *Gene ontology: tool for the unification of biology. The Gene Ontology Consortium.* Nat Genet, 2000. **25**(1): p. 25-9.
17. Karlsson, C., et al., *Genome-wide expression profiling reveals new candidate genes associated with osteoarthritis.* Osteoarthritis Cartilage, 2010. **18**(4): p. 581-92.

561 18. Varela-Eirin, M., et al., *Targeting of chondrocyte plasticity via connexin43 modulation*
562 *attenuates cellular senescence and fosters a pro-regenerative environment in*
563 *osteoarthritis.* Cell Death Dis, 2018. **9**(12): p. 1166.
564 19. Lesage, R., et al., *An integrated in silico-in vitro approach for*
565 *identification of therapeutic drug targets for osteoarthritis.* bioRxiv, 2021: p.
566 2021.09.27.461207.
567 20. Choi, Y., et al., *Discovery and structural analysis of Eph receptor tyrosine kinase*
568 *inhibitors.* Bioorg Med Chem Lett, 2009. **19**(15): p. 4467-70.
569 21. Moccia, M., et al., *Identification of Novel Small Molecule Inhibitors of Oncogenic RET*
570 *Kinase.* PLoS One, 2015. **10**(6): p. e0128364.
571 22. Libermann, T.A. and D. Baltimore, *Activation of interleukin-6 gene expression*
572 *through the NF-kappa B transcription factor.* Mol Cell Biol, 1990. **10**(5): p. 2327-34.
573 23. Mueller, M.B. and R.S. Tuan, *Functional characterization of hypertrophy in*
574 *chondrogenesis of human mesenchymal stem cells.* Arthritis Rheum, 2008. **58**(5): p.
575 1377-88.
576 24. Farrell, E., et al., *Chondrogenic priming of human bone marrow stromal cells: a better*
577 *route to bone repair?* Tissue Eng Part C Methods, 2009. **15**(2): p. 285-95.
578 25. Scotti, C., et al., *Recapitulation of endochondral bone formation using human adult*
579 *mesenchymal stem cells as a paradigm for developmental engineering.* Proc Natl
580 Acad Sci U S A, 2010. **107**(16): p. 7251-6.
581 26. Hellingman, C.A., et al., *Fibroblast growth factor receptors in in vitro and in vivo*
582 *chondrogenesis: relating tissue engineering using adult mesenchymal stem cells to*
583 *embryonic development.* Tissue Eng Part A, 2010. **16**(2): p. 545-56.
584 27. Narcisi, R., et al., *Long-term expansion, enhanced chondrogenic potential, and*
585 *suppression of endochondral ossification of adult human MSCs via WNT signaling*
586 *modulation.* Stem Cell Reports, 2015. **4**(3): p. 459-72.
587 28. van der Kraan, P.M., et al., *Development of osteoarthritic lesions in mice by*
588 *"metabolic" and "mechanical" alterations in the knee joints.* Am J Pathol, 1989.
589 **135**(6): p. 1001-14.
590 29. Zhang, H., D. Cai, and X. Bai, *Macrophages regulate the progression of osteoarthritis.*
591 Osteoarthritis Cartilage, 2020. **28**(5): p. 555-561.
592 30. Ferrao Blanco, M.N., et al., *Intra-articular injection of triamcinolone acetonide*
593 *sustains macrophage levels and aggravates osteophytosis during degenerative joint*
594 *disease in mice.* Br J Pharmacol, 2021.
595 31. Miller, R.E., R.J. Miller, and A.M. Malfait, *Osteoarthritis joint pain: the cytokine*
596 *connection.* Cytokine, 2014. **70**(2): p. 185-93.
597 32. Amato, K.R., et al., *EPHA2 Blockade Overcomes Acquired Resistance to EGFR Kinase*
598 *Inhibitors in Lung Cancer.* Cancer Res, 2016. **76**(2): p. 305-18.
599 33. Amato, K.R., et al., *Genetic and pharmacologic inhibition of EPHA2 promotes*
600 *apoptosis in NSCLC.* J Clin Invest, 2014. **124**(5): p. 2037-49.
601 34. Martini, G., et al., *EPHA2 Is a Predictive Biomarker of Resistance and a Potential*
602 *Therapeutic Target for Improving Antiepidermal Growth Factor Receptor Therapy in*
603 *Colorectal Cancer.* Mol Cancer Ther, 2019. **18**(4): p. 845-855.
604 35. Xiang, Y.P., et al., *Y772 phosphorylation of EphA2 is responsible for EphA2-dependent*
605 *NPC nasopharyngeal carcinoma growth by Shp2/Erk-1/2 signaling pathway.* Cell
606 Death Dis, 2020. **11**(8): p. 709.

607 36. Zeng, L., et al., *A Novel EphA2 Inhibitor Exerts Beneficial Effects in PI-IBS in Vivo and*
608 *in Vitro Models via Nrf2 and NF-kappaB Signaling Pathways.* Front Pharmacol, 2018.
609 **9**: p. 272.
610 37. Yan, D., et al., *Fibroblast growth factor receptor 1 is principally responsible for*
611 *fibroblast growth factor 2-induced catabolic activities in human articular*
612 *chondrocytes.* Arthritis Res Ther, 2011. **13**(4): p. R130.
613 38. Li, K., et al., *Tyrosine kinase Fyn promotes osteoarthritis by activating the beta-*
614 *catenin pathway.* Ann Rheum Dis, 2018. **77**(6): p. 935-943.
615 39. Zhang, X., R. Crawford, and Y. Xiao, *Inhibition of vascular endothelial growth factor*
616 *with shRNA in chondrocytes ameliorates osteoarthritis.* J Mol Med (Berl), 2016. **94**(7):
617 p. 787-98.
618 40. Ferrao Blanco, M.N., et al., *Tyrosine kinases regulate chondrocyte hypertrophy:*
619 *promising drug targets for Osteoarthritis.* Osteoarthritis Cartilage, 2021. **29**(10): p.
620 1389-1398.
621 41. Hunter, D.J., *Pharmacologic therapy for osteoarthritis--the era of disease*
622 *modification.* Nat Rev Rheumatol, 2011. **7**(1): p. 13-22.
623 42. Yahara, Y., et al., *Pterosin B prevents chondrocyte hypertrophy and osteoarthritis in*
624 *mice by inhibiting Sik3.* Nat Commun, 2016. **7**: p. 10959.
625 43. Carlson, E.L., et al., *Paroxetine-mediated GRK2 inhibition is a disease-modifying*
626 *treatment for osteoarthritis.* Sci Transl Med, 2021. **13**(580).
627 44. Roemer, F.W., et al., *The role of radiography and MRI for eligibility assessment in*
628 *DMOAD trials of knee OA.* Nat Rev Rheumatol, 2018. **14**(6): p. 372-380.
629 45. Sellam, J. and F. Berenbaum, *The role of synovitis in pathophysiology and clinical*
630 *symptoms of osteoarthritis.* Nat Rev Rheumatol, 2010. **6**(11): p. 625-35.
631 46. Hong, H.N., et al., *Cancer-associated fibroblasts promote gastric tumorigenesis*
632 *through EphA2 activation in a ligand-independent manner.* J Cancer Res Clin Oncol,
633 2018. **144**(9): p. 1649-1663.
634 47. Finney, A.C., et al., *EphA2 Expression Regulates Inflammation and Fibroproliferative*
635 *Remodeling in Atherosclerosis.* Circulation, 2017. **136**(6): p. 566-582.
636

637

638